

Anticoincidence measurement of ^{57}Fe Mössbauer spectra obtained after ^{57}Mn implantation: application to Fe in $\alpha\text{-Al}_2\text{O}_3$

**Y. Kobayashi · T. Nagatomo · Y. Yamada ·
M. Mihara · W. Sato · J. Miyazaki · S. Sato ·
A. Kitagawa · M. K. Kubo**

Published online: 21 January 2011
© Springer Science+Business Media B.V. 2011

Abstract A new detection system was developed using a gas-filled resonance counter operated in anticoincidence with a plastic scintillation detector for ^{57}Fe Mössbauer spectroscopy using a short-lived ^{57}Mn ($T_{1/2} = 1.45$ min) beam. We have succeeded in measuring ^{57}Fe Mössbauer spectra obtained after ^{57}Mn implantation into single-crystalline $\alpha\text{-Al}_2\text{O}_3$ at 92, 193, and 298 K, with an adequate ratio of the resonance peak against the background by applying this detection system, in spite of the extremely low implantation dose. Final positions of Fe atoms in $\alpha\text{-Al}_2\text{O}_3$ are discussed and compared with the results of the *ab initio* density functional calculations.

Keywords ^{57}Fe Mössbauer spectroscopy · Radioactive ^{57}Mn beam · Anticoincidence method · $\alpha\text{-Al}_2\text{O}_3$ · Projectile fragmentation reaction

Y. Kobayashi (✉) · T. Nagatomo
Advanced Meson Science Lab., Nishina Center for Accelerator-Based Science, RIKEN, Wako,
Saitama 351-0198, Japan
e-mail: kyoshio@riken.jp

T. Nagatomo · M. K. Kubo
International Christian University, Mitaka, Tokyo 181-8585, Japan

Y. Yamada
Department of Chemistry, Tokyo University of Science, Shinjuku, Tokyo 162-8601, Japan

M. Mihara
Graduate School of Science, Osaka University, Toyonaka, Osaka 560-0043, Japan

W. Sato
Department of Chemistry, Kanazawa University, Kanazawa, Ishikawa 920-1192, Japan

J. Miyazaki
College of Industrial Technology, Nihon University, Narashino, Chiba 275-8575, Japan

S. Sato · A. Kitagawa
National Institute of Radiological Science (NIRS), Inage, Chiba 263-8555, Japan

1 Introduction

Mössbauer emission spectroscopy provides us with unique information for characterization of extremely dilute atoms in materials. A lot of emission studies have been performed by chemical doping and low-energy ion-implantation of Mössbauer active probes [1]. ^{57}Co has been used conventionally and widely as a typical mother probe for ^{57}Fe Mössbauer spectroscopy in comparison with the seldomly used short-lived ^{57}Mn ($T_{1/2} = 1.45$ min) parent nuclide, as shown in Fig. 1. Recently, short-lived radioactive isotopes produced as secondary beams (RI beams) by ISOL method and projectile fragmentation have been available at several facilities in the world [2]. The RI beams acquire an increasing importance in materials science. Their intensities are considerably increasing and the implantation energies extending up to a GeV region are by several orders of magnitude higher than those available in the conventional ion implantation techniques. It is therefore important to establish a highly-efficient detector system in the on-line measurement of ^{57}Fe Mössbauer spectra using the short-lived ^{57}Mn beam.

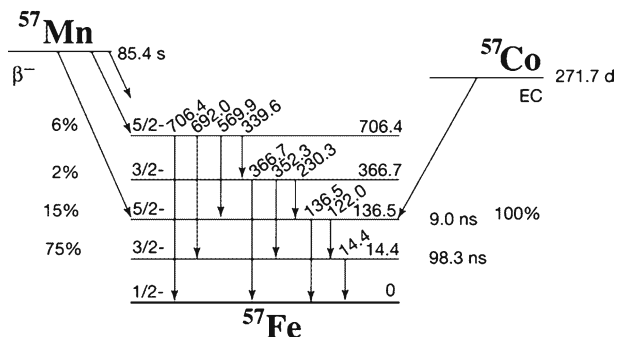
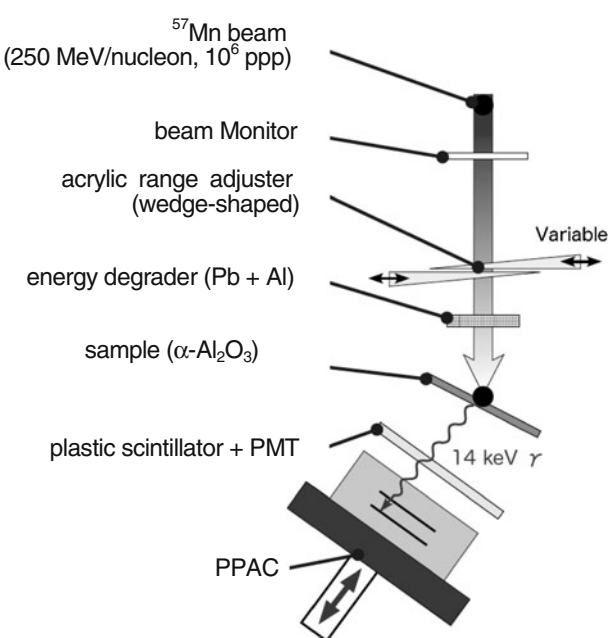
A gas-filled resonant detector, a so-called parallel-plate avalanche counter (PPAC), has been used exclusively in the ^{57}Fe Mössbauer spectroscopy combined with ^{57}Mn implantation [3] and Coulomb excitation [4]. The parallel plates in the PPAC consist of a cathode of an ^{57}Fe containing Mössbauer absorber and an anode of carbon, the electronic avalanches being released by gas ionization in the gap between these plates. The PPAC can collect effectively Mössbauer γ -quanta by accumulating the conversion electrons emitted by Mössbauer effect [5, 6]. However, ^{57}Mn nuclei β -decay to ^{57}Fe by emitting high-energy electrons. The electrons penetrating the PPAC cause the background level of the spectrum to increase, because the PPAC has very poor energy resolution. It has been possible to reduce the background by using an anticoincidence method between the β -ray and the Mössbauer γ -ray originated from ^{57}Mn .

In this paper, we describe a new detection system using the PPAC operated in anticoincidence with a plastic scintillation detector, and the application of this detector system to the study of Fe atoms arising from ^{57}Mn in single-crystalline $\alpha\text{-Al}_2\text{O}_3$. The present result is discussed on the base of the density functional calculations.

2 Experimental

(1) Production and implantation of ^{57}Mn probes

The experiment was carried out at the heavy-ion-synchrotron accelerator at the Heavy-Ion Medical Accelerator in Chiba (HIMAC) at the National Institute of Radiological Sciences (NIRS) [7]. ^{57}Mn nuclei were produced by the projectile fragmentation reaction of a primary beam of ^{58}Fe ions with the energy of 500 MeV/nucleon and a production target of ^9Be atoms with a thickness of 27 mm. The primary beam was supplied as a 250-ms pulsed beam every 3.3 s in the synchrotron. ^{57}Mn ions were separated after the fragment reaction and optimized electromagnetically by an in-flight RI beam separator of HIMAC. The purity of ^{57}Mn was more than 90% of the secondary beam after passing through the separator. The typical intensity and the energy of the ^{57}Mn beam before passing through the energy degraders were about

Fig. 1 Simplified decay scheme of ^{57}Fe **Fig. 2** Experimental setup of the ^{57}Fe Mössbauer spectroscopy using ^{57}Mn implantation with anticoincidence method

1.2×10^6 particles per pulsed-beam (ppp) and 250 MeV/nucleon, respectively. A Pb plate with the thickness of 4 mm, an Al plate with the thickness of 4 mm, and a couple of wedge-shaped acrylics were employed as energy degraders to stop all the ^{57}Mn nuclei at adequate depth in the sample. The single-crystalline $\alpha\text{-Al}_2\text{O}_3$ ($50 \times 50 \times 5$ mm, Furuuchi Chem.) was used as the sample, and was mounted on the cold finger of a cryostat. Typical implantation dose rate of ^{57}Mn was estimated to be 1×10^4 particles/(cm^2 s) into $\alpha\text{-Al}_2\text{O}_3$.

(2) $^{57}\text{Fe} (\leftarrow ^{57}\text{Mn})$ Mössbauer measurements using the anticoincidence method

A simplified experimental setup is shown in Fig. 2. The detection system consists of the parallel-plate avalanche counter (PPAC) and the anticoincidence thin plastic scintillator. The PPAC is equipped with an electrode made from ^{57}Fe -enriched stainless steel, and detects internal conversion electrons emitted after resonant

absorption of the Mössbauer γ -rays of ^{57}Fe arising from ^{57}Mn . A plastic scintillator was used to detect energetic electrons emitted from β^- -decay of ^{57}Mn , and was placed between the sample and the PPAC. The geometry of the scintillator ($80 \times 80 \times 0.5$ mm, BC-400, Bicron) was large enough to cover the detection area of the PPAC, and thin enough not to disturb the 14.4-keV radiation. This counter possesses a large β -ray detection efficiency of 98% by utilizing an adiabatic light guide designed to have a good photon transmission to a photomultiplier tube (R329-02, Hamamatsu). In this configuration, the detector system allows the on-line measurements of Mössbauer spectra using β -anticoincidence. A more detailed experimental setup will be explained in Ref. [8].

The PPAC was mounted on the Mössbauer driving unit (Wissel, MVT-1000). Velocity calibration of the system was carried out using a source of ^{57}Co embedded in Fe foil.

3 Results and discussion

The stopping range and longitudinal straggling width of ^{57}Mn probes with the energy of 250 MeV/nucleon in $\alpha\text{-Al}_2\text{O}_3$ were estimated to be 250 μm from the surface of the $\alpha\text{-Al}_2\text{O}_3$ sample and 200 μm , respectively. Since the implantation fluence of ^{57}Mn probes was extremely low ($\sim 10^6$ ppp), they could be considered completely isolated in $\alpha\text{-Al}_2\text{O}_3$.

The number of the PPAC signals gated with the anticoincidence detector was 24,261 events among the total events of 338,209 for a measuring period of 3 h at 298 K. The rejection efficiency of β -rays was consequently estimated to be more than 92%. The number of the PPAC signals was thus drastically reduced by the anticoincidence measurement. However, since the gated signals were “true”, the anticoincidence method improved the quality of the spectrum despite the measuring time of 3 h and the low implantation dose rate of about 10^4 particles/ $(\text{cm}^2 \text{s})$.

The ^{57}Fe Mössbauer spectra of ^{57}Mn implanted into $\alpha\text{-Al}_2\text{O}_3$ by anticoincidence method were measured at 92, 193, and 298 K. Figure 3 shows the typical ^{57}Fe ($\leftarrow^{57}\text{Mn}$) Mössbauer spectrum of $\alpha\text{-Al}_2\text{O}_3$ obtained at 298 K. The isomer shift is given relative to Fe metal at room temperature. The Mössbauer parameters were determined by a least-squares fitting procedure assuming Lorentzian line-shape. The Mössbauer spectra taken with $\alpha\text{-Al}_2\text{O}_3$ at 3 temperatures between 92 K and room temperature could be analyzed by three components of symmetrical doublets D1, D2, and D3. There was no obvious magnetic splitting in all the obtained spectra. The area intensities of these three components at 92 K were almost equivalent, but D1 increased gradually with increasing temperature. The derived Mössbauer parameters are summarized in Table 1.

The electronic structures of Fe atoms in aluminum oxide clusters ($\text{Fe}@Al_n O_m$) were calculated by using the *ab initio* ORCA program (ver. 2.6.35) developed by F. Neese and co-workers [9]. The molecular structures of aluminum oxide clusters were optimized varying the positions of six oxygen atoms coordinating to Fe atoms using the B3LYP/TZVP density functional calculation. For example, $\text{Fe}@Al_{13}O_{21}$ means a model cluster where a Fe atom is substituting an original Al^{3+} site in the corundum structure of $\alpha\text{-Al}_2\text{O}_3$. The electron density and the electric field gradient in various clusters of $\text{Fe}@Al_n O_m$ were calculated by the ORCA program. The obtained

Fig. 3 ^{57}Fe Mössbauer spectrum of ^{57}Mn implanted in $\alpha\text{-Al}_2\text{O}_3$ at 298 K

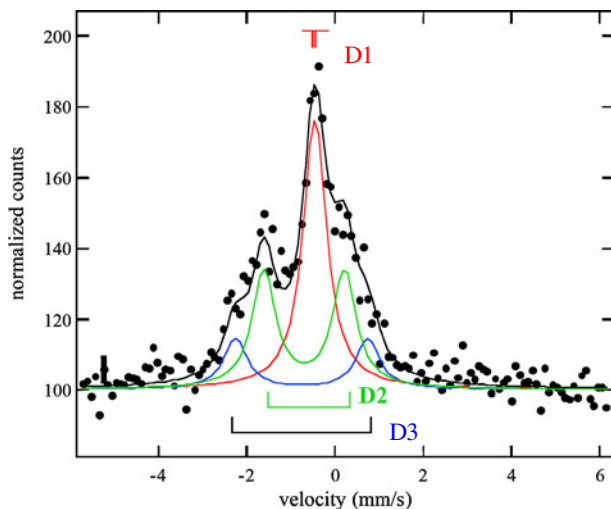


Table 1 Mössbauer parameters of ^{57}Mn implanted into $\alpha\text{-Al}_2\text{O}_3$

| Temp. (K) | D1 | | D2 | | D3 | |
|----------------------|-----------------|---------------------|-----------------|---------------------|-----------------|---------------------|
| | δ (mm/s) | ΔE_Q (mm/s) | δ (mm/s) | ΔE_Q (mm/s) | δ (mm/s) | ΔE_Q (mm/s) |
| 92 | 0.61(3) | 0.65(5) | 0.75(2) | 2.00(5) | 0.91(3) | 3.53(7) |
| 193 | 0.53(3) | 0.47(7) | 0.75(5) | 1.70(7) | 0.80(3) | 2.96(6) |
| 298 | 0.43(2) | 0.22(7) | 0.70(3) | 1.31(7) | 0.68(2) | 2.43(5) |
| Calc. by ORCA [6, 7] | 0.486 | 0.309 | 0.695 | 1.350 | 0.768 | 2.409 |

values by the ORCA program were converted into the values of *I.S.* and *Q.S.* [10]. Compared with the derived Mössbauer parameters at room temperature, D1 and D2 doublets correspond approximately to $\text{Fe@Al}_{13}\text{O}_{21}$ and $\text{Fe@Al}_8\text{O}_{12}$ clusters. Fe is found to be in high-spin Fe^{3+} at the substitutional Al sites in $\alpha\text{-Al}_2\text{O}_3$, and Fe^{II} at the interstitial sites surrounded with octahedral O_6 symmetry, respectively. D3 doublet is corresponding to $\text{Fe@Al}_{13}\text{O}_{20}$, and assigned to Fe^{II} at a substitutional Al site with an oxygen deficiency. The present result is consistent in principle with the results at room temperature reported by Dézsi and co-workers [11]. The temperature dependence of the relative intensities in this study suggests that the lattice defects gradually recover with an increase of temperature. It is concluded that the anticoincidence detector system is very useful for the measurement of ^{57}Fe Mössbauer spectra obtained after dilute ^{57}Mn implantation. Further implantation experiments over a wide temperature range will be carried out to elucidate the site assignments of extremely dilute Fe atoms in $\alpha\text{-Al}_2\text{O}_3$.

4 Conclusion

The detection system using the anticoincidence method between Mössbauer γ -rays and high-energy β -rays emitted from short-lived ^{57}Mn nuclei was newly developed. We succeeded in measuring ^{57}Fe Mössbauer spectra obtained after ^{57}Mn

implantation in $\alpha\text{-Al}_2\text{O}_3$ with an adequate ratio of the resonance peak against the background by applying the anticoincidence measurement in spite of the extremely low ^{57}Mn implantation dose. The Mössbauer spectra measured at 92 K, 193 K, and 298 K could be analyzed by three components of symmetrical doublets. There was not any significant magnetic splitting in this temperature region. On the basis of the density functional calculation, these components were assigned to Fe^{3+} at the substitutional Al^{3+} sites in $\alpha\text{-Al}_2\text{O}_3$, to interstitial Fe atoms surrounded with octahedral O_6 symmetry, and to Fe atoms at a substitutional Al^{3+} sites with an oxygen deficiency.

Acknowledgements This work was carried out as a part of Research Project with Heavy Ions at NIRS-HIMAC under the contract of and partial support by Support Program for Private Universities (S0801012) from the Ministry of Education, Culture, Sports, Science and Technology, Japan. We are thankful to Dr. N. Suzuki and Dr. S. Kamiguchi of Chemical Analysis Team in RIKEN for production of ^{58}Fe -enriched ferrocene as an ion source.

References

1. de Waard, H., Niesen, L.: Ion implantation Mössbauer effect studies. In: Mössbauer Spectroscopy Applied to Inorganic Chemistry, vol. 2, p. 1. Plenum, New York (1987)
2. Kluge, H.-J.: Hyp. Int. **196**, 295–337 (2009)
3. Mølholt, T.E., Mantovan, R., Gunnlaugsson, H.P., Bharuth-Ram, K., Fanciulli, M., Gíslason, H.P., Johnston, K., Kobayashi, Y., Langouche, G., Masenda, H., Naidoo, D., Ólafsson, S., Sielemann, R., Weyer, G.: Physica, B **404**, 4820–4822 (2009)
4. Sielemann, R., Kobayashi, Y., Yoshida, Y., Gunnlaugsson, H.P., Weyer, G.: Phys. Rev. Lett. **101**, 1372061–1372064 (2008)
5. Weyer, G.: Applications of parallel-plate avalanche counters in Mössbauer spectroscopy. In: Mössbauer Effect Methodology, p. 301. Plenum, New York (1976)
6. Saito, T., Kobayashi, Y., Kubo, M.K., Yamada, Y.: J. Radioanal. Nucl. Chem. **255**, 519–522 (2003)
7. Hirao, Y., Ogawa, H., Yamada, S., Sato, Y., Yamada, T., Sato, K., Itano, A., Kanazawa, M., Noda, K., Kawachi, K., Endo, M., Kanai, T., Kohno, T., Sudou, M., Minohara, S., Kitagawa, A., Soga, F., Takada, E., Watanabe, S., Endo, K., Kumada, M., Matsumoto, S.: Nucl. Phys., A **538**, 541–550 (1992)
8. Nagatomo, T., Kobayashi, Y., Kubo, M.K., Yamada, Y., Mihara, M., Sato, W., Miyazaki, J., Sato, S., Kitagawa, A.: Nucl. Instrum. Methods, B (2010). doi:[10.1016/j.nimb.2010.12.042](https://doi.org/10.1016/j.nimb.2010.12.042)
9. See web: <http://www.thch.uni-bonn.de/tc/orca>
10. Römel, M., Ye, S., Neese, F.: Inorg. Chem. **48**, 784–785 (2009)
11. Dézsi, I., Szúcs, I., Fetzer, C., Pattyn, H., Langouche, G., Pfannes, H.D., Magalhaes-Paniago, R.: J. Phys.: Cond. Matt. **12**, 2291–2296 (2000)